

Quantum Teleportation with a Complete Bell State Measurement

Yoon-Ho Kim,* Sergei P. Kulik,† and Yanhua Shih

Department of Physics, University of Maryland, Baltimore County, Baltimore, Maryland 21250

(Submitted to PRL)

We report a quantum teleportation experiment in which nonlinear interactions are used for the Bell state measurements. The experimental results demonstrate the working principle of irreversibly teleporting an unknown arbitrary quantum state from one system to another distant system by disassembling into and then later reconstructing from purely classical information and nonclassical EPR correlations. The distinct feature of this experiment is that *all* four Bell states can be distinguished in the Bell state measurement. Teleportation of a quantum state can thus occur with certainty in principle.

PACS Number: 03.65.Bz, 03.67.Hk, 42.50.Dv, 42.65.Ky

The idea of quantum teleportation is to utilize the non-local correlations between an Einstein-Podolsky-Rosen pair of particles [1] to prepare a quantum system in some state, which is the exact replica of an arbitrary unknown state of a distant individual system [2]. Three experiments in this direction were published recently [3–5].

The following conditions must be satisfied in any claim for quantum teleportation: (i) the input quantum state, which is teleported in the experiment must be an *arbitrary* state, (ii) there must be an output quantum state which is an “instantaneous copy” of the input quantum state, and (iii) the Bell state measurement (BSM) must be able to distinguish the complete set of the orthogonal Bell states so that the input state can be teleported with certainty.

In this Letter, we experimentally demonstrate a quantum teleportation scheme which satisfies all three of the above conditions. The input state is an *arbitrary polarization state* and the BSM can distinguish *all* four orthogonal Bell states so that the state has a 100% certainty to be teleported in principle. This is because the BSM is based on nonlinear interactions which are *necessary* and *non-trivial* physical processes for correlating the input state and the entangled EPR pair [6,7].

The basic elements of the experiment are schematically shown in Fig. 1. Just as the original proposal of quantum teleportation [2], it consists of four essential parts: (a) the input state, (b) the EPR pair, (c) Alice (who performs the BSM of the input state and her EPR particle), and (d) Bob (who carries out unitary operations on his EPR particle). The input quantum state is an *arbitrary polarization state* given by,

$$|\Psi_1\rangle = \alpha|0_1\rangle + \beta|1_1\rangle, \quad (1)$$

where $|0\rangle$ and $|1\rangle$ represent the two orthogonal linear polarization bases (specifically in this paper) $|H\rangle$ (horizontal) and $|V\rangle$ (vertical) respectively. α and β are two arbitrary complex amplitudes with respect to the $|0\rangle$ and

$|1\rangle$ bases and they satisfy the condition $|\alpha|^2 + |\beta|^2 = 1$. The EPR pair shared by Alice and Bob is prepared by spontaneous parametric down conversion (SPDC) as,

$$|\Psi_{23}\rangle = \frac{1}{\sqrt{2}}\{|0_20_3\rangle - |1_21_3\rangle\}, \quad (2)$$

with the subscripts 2 and 3 as labeled in Fig.1 [8]. The complete state of the three particles before Alice’s measurement is then,

$$\begin{aligned} |\Psi_{123}\rangle = & \frac{\alpha}{\sqrt{2}}\{|0_10_20_3\rangle - |0_11_21_3\rangle\} \\ & + \frac{\beta}{\sqrt{2}}\{|1_10_20_3\rangle - |1_11_21_3\rangle\}. \end{aligned} \quad (3)$$

The four Bell states which form a complete orthonormal basis for both particle 1 and particle 2 are usually represented as,

$$\begin{aligned} |\Phi_{12}^{(\pm)}\rangle &= \frac{1}{\sqrt{2}}\{|0_10_2\rangle \pm |1_11_2\rangle\}, \\ |\Psi_{12}^{(\pm)}\rangle &= \frac{1}{\sqrt{2}}\{|0_11_2\rangle \pm |1_10_2\rangle\}. \end{aligned}$$

State (3) can now be re-written in the following form based on the above orthonormal Bell states,

$$\begin{aligned} |\Psi_{123}\rangle = \frac{1}{2}\{ & |\Phi_{12}^{(+)}\rangle (\alpha|0_3\rangle - \beta|1_3\rangle) \\ & + |\Phi_{12}^{(-)}\rangle (\alpha|0_3\rangle + \beta|1_3\rangle) \\ & + |\Psi_{12}^{(+)}\rangle (-\alpha|1_3\rangle + \beta|0_3\rangle) \\ & + |\Psi_{12}^{(-)}\rangle (-\alpha|1_3\rangle - \beta|0_3\rangle) \}. \end{aligned} \quad (4)$$

To teleport the state of particle 1 to particle 3 reliably, Alice must be able to distinguish her four Bell states by means of the BSM performed on particle 1 and her EPR particle (particle 2). She then tells Bob through a classical channel to perform a corresponding linear unitary operation on his EPR particle (particle 3) to obtain an exact replica of the state of particle 1. This completes the process of quantum teleportation.

The distinct feature of the scheme shown in Fig.1 is that the BSM is based on nonlinear interactions: optical Sum Frequency Generation (SFG) (or “upconversion”). Four SFG nonlinear crystals are used for “measuring”

*Email: yokim@umbc.edu

†Permanent Address: Department of Physics, Moscow State University, Moscow, Russia

and “distinguishing” the complete set of the four Bell states. Photon 1 and photon 2 may interact either in the two type-I crystals or in the two type-II crystals to generate a higher frequency photon (labeled as photon 4). The projection measurements on photon 4 (either at the 45° or at the 135° direction) correspond to the four Bell states of photon 1 and photon 2, $|\Phi_{12}^{(\pm)}\rangle$ and $|\Psi_{12}^{(\pm)}\rangle$.

Let us now discuss the BSM in detail (see Fig.1). The first type-I SFG crystal converts two $|V\rangle$ polarized photons $|1_1 1_2\rangle$ into a single horizontal polarized photon $|H_4\rangle$. Likewise, the second type-I SFG crystal converts two $|H\rangle$ polarized photons $|0_1 0_2\rangle$ into a single vertical polarized photon $|V_4\rangle$. The first and the last terms on the right-hand side in Eq.(3) thus become,

$$|\Psi_{43}\rangle = \alpha|V_4 0_3\rangle - \beta|H_4 1_3\rangle.$$

Dichroic beamsplitter M reflects only SFG photons to the 45° polarization projector G_1 . Two detectors D_4^I and D_4^{II} are placed at the 45° and 135° output ports of G_1 respectively. Denoting the 45° and 135° polarization bases by $|45^\circ\rangle$ and $|135^\circ\rangle$, the state $|\Psi_{43}\rangle$ may be rewritten as,

$$|\Psi_{43}\rangle = \frac{1}{\sqrt{2}}\{|45^\circ\rangle_4(\alpha|0_3\rangle - \beta|1_3\rangle) + |135^\circ\rangle_4(\alpha|0_3\rangle + \beta|1_3\rangle)\}, \quad (5)$$

which gives,

$$\begin{aligned} |\Psi\rangle_{3|D_4^I} &= \alpha|0_3\rangle - \beta|1_3\rangle, \\ |\Psi\rangle_{3|D_4^{II}} &= \alpha|0_3\rangle + \beta|1_3\rangle, \end{aligned} \quad (6)$$

i.e., if detector D_4^I (45°) is triggered, the quantum state of Bob’s EPR photon (photon 3) is:

$$|\Psi_3\rangle = \alpha|0_3\rangle - \beta|1_3\rangle,$$

and, if detector D_4^{II} (135°) is triggered, the quantum state of Bob’s photon is:

$$|\Psi_3\rangle = \alpha|0_3\rangle + \beta|1_3\rangle.$$

As we have analyzed above, the 45° and the 135° polarized type-I SFG components in Eq.(5) correspond to the superposition of $|0_1 0_2\rangle$ and $|1_1 1_2\rangle$ which are the respective Bell states $|\Phi_{12}^{(+)}\rangle$ and $|\Phi_{12}^{(-)}\rangle$.

Similarly, the other two Bell states are distinguished by the type-II SFG’s. The states $|0_1 1_2\rangle$ and $|1_1 0_2\rangle$ are made to interact in the first and the second type-II SFG crystals respectively to generate a higher frequency photon with either horizontal (the first type-II SFG) or vertical (the second type-II SFG) polarization. A 45° polarization projector G_2 is used after the type-II SFG crystals and two detectors D_4^{III} and D_4^{IV} are placed at the 45° and the 135° output ports of G_2 respectively. On the

new bases of 45° and 135° for the SFG photon, the second and the third terms on the right-hand side in Eq.(3) thus become,

$$|\Psi_{43}\rangle = \frac{1}{\sqrt{2}}\{|45^\circ\rangle_4(-\alpha|1_3\rangle + \beta|0_3\rangle) + |135^\circ\rangle_4(-\alpha|1_3\rangle - \beta|0_3\rangle)\}, \quad (7)$$

which gives,

$$\begin{aligned} |\Psi\rangle_{3|D_4^{III}} &= -\alpha|1_3\rangle + \beta|0_3\rangle, \\ |\Psi\rangle_{3|D_4^{IV}} &= -\alpha|1_3\rangle - \beta|0_3\rangle, \end{aligned} \quad (8)$$

i.e., if detector D_4^{III} (45°) is triggered, the quantum state of Bob’s photon is:

$$|\Psi_3\rangle = -\alpha|1_3\rangle + \beta|0_3\rangle,$$

and if detector D_4^{IV} (135°) is triggered, the quantum state of Bob’s photon is:

$$|\Psi_3\rangle = -\alpha|1_3\rangle - \beta|0_3\rangle.$$

The 45° and the 135° polarized type-II SFG components correspond to the superposition of $|0_1 1_2\rangle$ and $|1_1 0_2\rangle$ which are the Bell states $|\Psi_{12}^{(+)}\rangle$ and $|\Psi_{12}^{(-)}\rangle$ respectively.

To obtain the exact replica of the state of Eq.(1), Bob needs simply to perform a corresponding unitary transformation after learning from Alice which of her four detectors, D_4^I , D_4^{II} , D_4^{III} , or D_4^{IV} , has triggered [9].

To demonstrate the working principle of this scheme, we measure the joint detection rates between detectors D_4^I - D_3 , D_4^{II} - D_3 , D_4^{III} - D_3 and D_4^{IV} - D_3 , where D_3 is Bob’s detector (see Fig.4). In these measurements we choose the input state $|\Psi_1\rangle$ as a linear polarization state. For a fixed input polarization state, the angle of the polarization analyzer A_3 which is placed in front of Bob’s detector is rotated and the joint detection rates are recorded. Figure 2 shows two typical data sets for D_4^I - D_3 and D_4^{II} - D_3 . The input polarization state is 45° . Clearly, these data curves confirm Eq.(6). The different phases of the two curves reflect the phase difference between the two states in Eq.(6). Experimental data for D_4^{III} - D_3 and D_4^{IV} - D_3 show similar behavior, see Fig. 3, which confirm Eq.(8).

We now discuss the details of the experimental setup. The schematic of the experimental setup is shown in Fig. 4. The input polarization state is prepared by using a $\lambda/2$ plate from a femtosecond laser pulse (pulse width ≈ 100 fsec and central wavelength = 800nm) [10]. The EPR pair (730nm-885nm photon pair) is generated by two non-degenerate type-I SPDC’s. The optical axes of the first and the second SPDC crystals are oriented in the respective horizontal (\odot) and vertical (\updownarrow) directions. The SPDC crystals are pumped by a 45° polarized 100fsec laser pulse with 400nm central wavelength. The BBO crystals (each with thickness 3.4mm) are cut for collinear non-degenerate phase matching. Since the two crystals

are pumped equally, the SPDC pair can be generated either in the first BBO as $|V_{885}/2\rangle|V_{730}\rangle_3$ ($|1_21_3\rangle$) or in the second BBO as $|H_{885}/2\rangle|H_{730}\rangle_3$ ($|0_20_3\rangle$) with equal probability (885 and 730 refer to the wavelengths in nanometer). In order to prepare an EPR state in the form of Eq.(2) (a Bell state), these two amplitudes have to be quantum mechanically “indistinguishable” and have the expected relative phase. A Compensator (C-1) is used for this purpose and it consists of two parts: a thick quartz rod and two thin plates. The thick quartz rod is used to compensate the time delay between the two amplitudes $|1_21_3\rangle$ and the $|0_20_3\rangle$, and two thin quartz plates are used to adjust the relative phase between them by angular tilting. A dichroic beamsplitter DBS is placed behind the SPDC crystals to separate and send the photon 2 (885nm) and photon 3 (730nm) to Alice and Bob respectively. To check the EPR state, a flipper mirror FM is used to send the photon 2 (885nm) to a photon-counting detector D_2 for EPR correlation measurement. Both the space-time and polarization correlations must be checked before teleportation measurements, in order to be certain of having high degree EPR entanglement and the expected relative phase between the $|1_21_3\rangle$ and the $|0_20_3\rangle$ amplitudes (see Ref. [11] for details). Once the EPR state in Eq.(2) is prepared, FM is flipped-down and photon 2 (885nm) is given to Alice for BSM with photon 1.

The BSM consists of four SFG nonlinear crystals, two 45° projectors (G_1 and G_2), four single photon counting detectors (D_4^I , D_4^{II} , D_4^{III} , and D_4^V) and two compensators as well as other necessary optical components. The input photon (800nm) and photon 2 (885nm) may either interact in the two type-I or in the two type-II SFG crystals. Two pairs of lenses (L) are used as telescopes to focus the input beams onto the crystals. The vertical (horizontal) polarized amplitudes of the input photon (800nm) and the vertical (horizontal) polarized photon 2 (885nm) interact in the first (second) type-I SFG to generate a 420nm horizontal (vertical) polarized photon [12]. The horizontal (vertical) polarized amplitudes of the input photon and the vertical (horizontal) polarized photon 2 interact in the first (second) type-II SFG to generate a 420nm horizontal (vertical) polarized photon. The 420nm photons generated in the type-I SFG process is reflected to detectors D_4^I and D_4^{II} (after passing through C-2 and a 45° polarization projector G_1) by a dichroic beamsplitter DBS_2 and similarly for the 420nm photons created in two type-II SFG processes. It is very important to design and adjust the Compensators (C-2 and C-3) correctly in order to make the horizontal and the vertical components of the 420nm SFG quantum mechanically indistinguishable and to attain the expected relative phase. These two compensators are similar to C-1.

Since the input state (photon 1) and photon 2 should overlap inside the SFG crystals exactly, a prism is used to adjust the path-length of the input pulse [13]. M_1 is a dichroic mirror which reflects the 800nm photons while

transmitting the 885nm ones. In order to be sure that the SFG process occurs with a single-photon input, we measured the coincidence counting rate between one of Alice’s detectors and Bob’s detector D_3 by moving the position of the prism. Fig. 5 shows a typical data curve of the measurement. It is clear that SFG only occurs when the input pulse (photon 1) and photon 2 (single-photon created by the SPDC process) overlap perfectly inside the SFG crystals [14].

Readers might have noticed that the efficiency in the teleportation measurement is a lot lower than the SFG demonstration. The reason why we get such a low coincidence counting rate in Figs.2 and 3 as compared to Fig.5 is that very small pinholes had to be placed in front of Alice’s detectors for the teleportation measurement to ensure good spatial mode overlap. The improvements of the SFG and the collection efficiencies while preserving good spatial mode overlap are now underway.

In summary, we have shown a proof-of-principle experimental demonstration of quantum teleportation with complete a Bell state measurement. The two main features lie at the heart of our scheme: (i) EPR-Bohm type quantum correlation and (ii) the BSM using nonlinear interactions. Single photon SFG is used as the BSM and the working principle is demonstrated by observing correlations between the joint measurement of Alice and Bob. In the current experiment, femtosecond laser pulses are used to prepare the input polarization state to reduce data collection time. Recent research on nonlinear optics at low light levels may enable high-efficiency SFG at single-photon level in the near future [15].

We would like to thank C.H. Bennett and M.H. Rubin for helpful discussions. This work was supported in part by the Office of Naval Research, ARDA, and the National Security Agency.

-
- [1] A. Einstein, B. Podolsky, and N. Rosen, Phys. Rev. **47**, 777 (1935).
 - [2] C.H. Bennett *et al.*, Phys. Rev. Lett. **70**, 1895 (1993).
 - [3] D. Bouwmeester *et al.*, Nature **390**, 575 (1997).
 - [4] D. Boschi *et al.*, Phys. Rev. Lett. **80**, 1121 (1998).
 - [5] A. Furusawa *et al.*, Science **282**, 706 (1998).
 - [6] L. Vaidman and N. Yoran, Phys. Rev. A **59**, 116 (1999); N. Lütkenhaus, J. Calsamiglia, and K.-A. Suominen, *ibid.* **59**, 3295 (1999).
 - [7] D.N. Klyshko, JETP **87**, 639 (1998).
 - [8] Note that any one of the four Bell states can be used for this purpose.
 - [9] Complete BSM using SFG is also useful for other applications, see C.H. Bennett and S.J. Wiesner, Phys. Rev. Lett. **69**, 2881 (1992).
 - [10] In this experiment, the input state is a polarization state of a femtosecond laser pulse. Only one out of approximately 10^{10} photons, all in the same polarization state, in each laser pulse is actually “upconverted” in the SFG process. It can be easily shown that each photon has the polarization state of Eq.(1) by considering the correspondence principle. What is being teleported is the state or

qubit associated with this photon. (Note, quantum teleportation does not teleport the “quantum” but rather, the state of the quantum). In principle, it does not prevent one to use a single-photon qubit as the input state in this experiment. Due to the low efficiency of SFG, one needs to wait a much longer time for teleportation to occur.

- [11] Y.-H. Kim, S.P. Kulik, and Y.H. Shih, Phys. Rev. A **62**, 011802(R), (2000); <http://arxiv.org/abs/quant-ph/0007067>.
- [12] Note that there are five different wavelengths which are tunable as long as the two phase matching conditions (for SPDC and for SFG) are satisfied. Also five independent relative phases which affect the output state can be varied.
- [13] 800nm input pulse and 400nm pump pulse (which pumps the SPDC crystals) are actually drawn from a single Ti:Sapphire laser to ensure that they have the same repetition period.
- [14] The efficiency of SFG (from the SPDC photons) is roughly estimated to be 0.1~1%. The SFG crystals used for the data shown in this paper are BBO’s with 2mm thickness.
- [15] S.E. Harris and L.V. Hau, Phys. Rev. Lett. **82**, 4611 (1999).

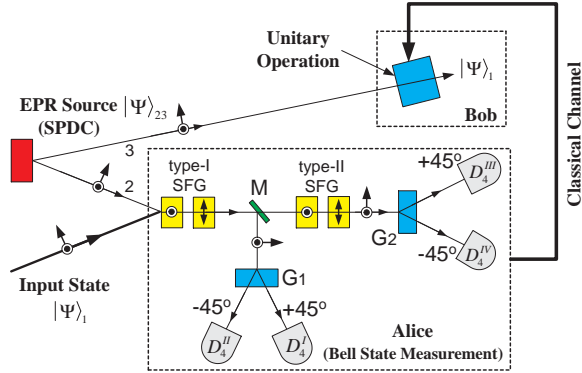


FIG. 1. Principle schematic of quantum teleportation with a complete BSM. Nonlinear interactions (SFG) are used to perform the BSM. \odot and \uparrow represent the respective horizontal and vertical orientations of the optic axes of the crystals.

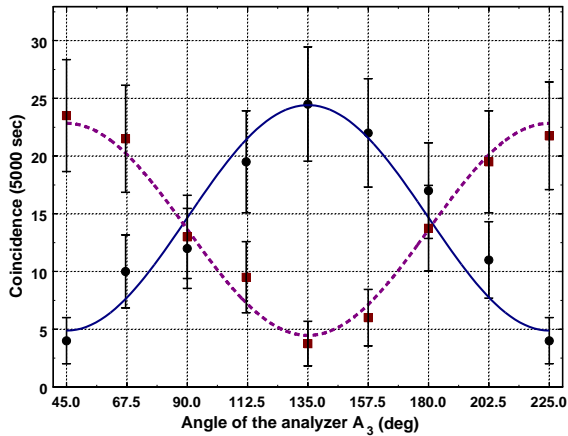


FIG. 2. Solid line (circled data points) is the joint detection rate $D_4^I - D_3$ for 45° linear polarization as an input state. Dashed line (square data points) is for $D_4^{II} - D_3$ for the same input state. The expected π phase shift is clearly demonstrated.

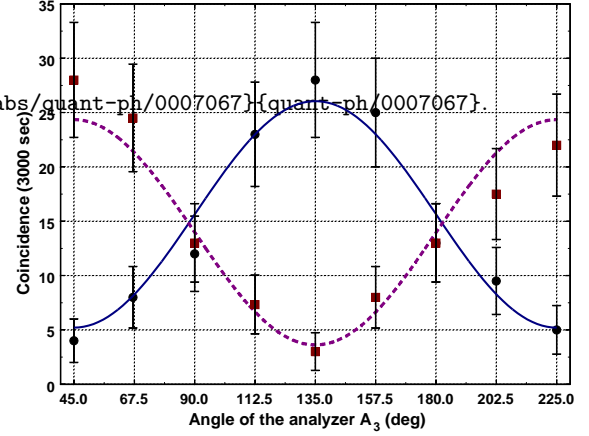


FIG. 3. Solid line (circled data points) is the joint detection rate $D_4^{III} - D_3$ and dashed line (square data points) is for $D_4^{IV} - D_3$. Again, the expected π phase shift is clearly demonstrated.

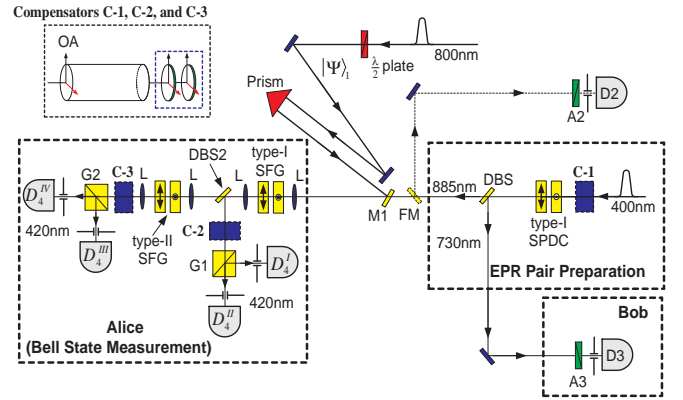


FIG. 4. Diagram of the experimental setup. The inset shows the details of the compensators. See text for details.

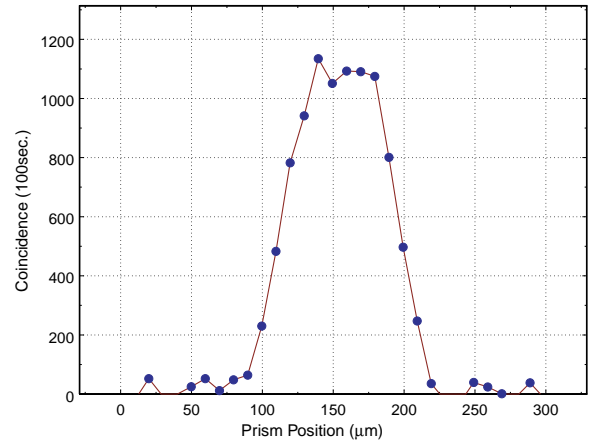


FIG. 5. SFG measurement as a function of the prism position. SFG is observed only when the input pulse and the SPDC photons overlap exactly inside the crystals.